

# SAM-VMNet: Deep Neural Networks For Coronary Angiography Vessel Segmentation

Xueying Zeng<sup>a</sup>, Baixiang Huang<sup>b</sup>, Yu Luo<sup>a</sup>, Guangyu Wei<sup>c</sup>, Songyan He<sup>a</sup>, Yushuang Shao<sup>d</sup>

<sup>a</sup>School of Mathematical Sciences, Ocean University of China, Qingdao, Shandong, China

<sup>b</sup>School of Management, Ocean University of China, Qingdao, Shandong, China

<sup>c</sup>School of Haide, Ocean University of China, Qingdao, Shandong, China

<sup>d</sup>School of ocean and atmosphere, Ocean University of China, Qingdao, Shandong, China

## Abstract

Coronary artery disease (CAD) is one of the most prevalent diseases in the cardiovascular field and one of the major contributors to death worldwide. Computed Tomography Angiography (CTA) images are regarded as the authoritative standard for the diagnosis of coronary artery disease, and by performing vessel segmentation and stenosis detection on CTA images, physicians are able to diagnose coronary artery disease more accurately. In order to combine the advantages of both the base model and the domain-specific model, and to achieve high-precision and fully-automatic segmentation and detection with a limited number of training samples, we propose a novel architecture, SAM-VMNet, which combines the powerful feature extraction capability of MedSAM with the advantage of the linear complexity of the visual state-space model of VM-UNet, giving it faster inferences than Vision Transformer with faster inference speed and stronger data processing capability, achieving higher segmentation accuracy and stability for CTA images. Experimental results show that the SAM-VMNet architecture performs excellently in the CTA image segmentation task, with a segmentation accuracy of up to 98.32% and a sensitivity of up to 99.33%, which is significantly better than other existing models and has stronger domain adaptability. Comprehensive evaluation of the CTA image segmentation task shows that SAM-VMNet accurately extracts the vascular trunks and capillaries, demonstrating its great potential and wide range of application scenarios for the vascular segmentation task, and also laying a solid foundation for further stenosis detection.

# 1. Introduction

Coronary artery disease (CAD) is the most common cardiovascular disease and is one of the most common causes of death in the world. In the latest data published by the World Health Organisation (WHO), cardiovascular disease is one of the four major non-communicable chronic diseases and the one with the highest increase in deaths<sup>1</sup>. The disease is characterised by the accumulation of plaque in the blood vessels, called Atherosclerosis, which leads to the narrowing and hardening of the blood vessels, resulting in ischaemic changes in tissues or organs, increasing the risk of angina pectoris, myocardial infarction and other cardiovascular events<sup>2</sup>.

Coronary angiography (CA) is considered the "gold standard" for diagnosing coronary artery disease (CAD) in clinical practice<sup>3</sup>, which can show the backbone of the left or right coronary artery and its branch vessels, and can be used to understand the presence of stenotic foci. Because coronary angiography images are complex, it is difficult to obtain clear subtracted images like brain and limb angiography images, so it is crucial to extract a clear and complete vascular tree structure from coronary angiography images.

Currently, there are many classical methods for arteriography image segmentation such as threshold segmentation<sup>4</sup>, Canny operator edge detection<sup>5</sup>, region growing<sup>6</sup>, and tracking-based methods<sup>7,8,9</sup>. However, since arteriography images usually have low contrast and complex backgrounds, traditional algorithms may be difficult to meet the clinical needs in practical applications. Therefore, many improved methods and new techniques, such as deep learning methods, have been proposed in recent years to increase the accuracy and robustness of arteriography image segmentation. Convolutional neural network (CNN) utilises a deep learning model to automatically extract features and retain high-resolution features through jump connections. It highlights the use of CNN architecture for segmenting blood vessels in time-of-flight magnetic resonance angiography (TOF MRA) images of healthy subjects, involving the extraction of 2D manually annotated image chunks in different orientations and using them as inputs for CNN training<sup>10</sup>. Among others, the convolutional neural network-based UNet<sup>11</sup> has been widely used in biomedical image segmentation tasks, where such networks can be trained end-to-end even with very few images and outperforms the best previous methods in the ISBI challenge of segmenting neural structures stacked in electron microscopes. Segment Anything Model (SAM)<sup>12</sup> as a large model for image segmentation based on Vision Transformer<sup>13</sup> for feature extraction has a strong generality as well as generalisation ability, which is designed to be cueable to migrate zero samples to new image distributions and tasks. Among them MedSAM<sup>14</sup> utilised this model on the basis of SAM in a data collection loop using one million medical images for training, which is better adapted to the characteristics of medical images. It shows great potential in medical image segmentation. Recently, Mamba model<sup>15</sup> is proposed as an emerging deep learning sequence architecture, which improves the traditional state space model by selective state space model with fast inference and linear scaling of sequence length, and its performance can be improved to one million length sequences on real data, which significantly improves the efficiency of processing long sequence data. The proposed VM-Unet<sup>16</sup> based on the Mamba model is more efficient in processing large-scale medical image data, which utilises the state space model,

in particular the Visual State Space (VSS) block, as a base block to capture a wide range of contextual information and constructs an asymmetric encoder-decoder structure. The results show that VM-UNet performs competitively in medical image segmentation tasks. However, the latest deep learning architectures still perform poorly when dealing with small vessels, severely stenotic vessels, or poor image quality<sup>17,18</sup>. In this study, we propose a new deep learning framework, SAM-VMNet, which achieves high-quality automatic segmentation of coronary angiography images by combining the advantages of VM-UNet and MedSAM. The main process is to use the Transformer module in SAM to extract global and local features in coronary angiography images; then the selective state space model in Mamba model is used to enhance the processing capability of long sequence data and improve the segmentation accuracy. Through comparison experiments as well as ablation experiments, SAM-VMNet outperforms the base model and other popular deep learning models in terms of segmentation accuracy and computational efficiency.

## II. Method

### II.A. Architecture Overview

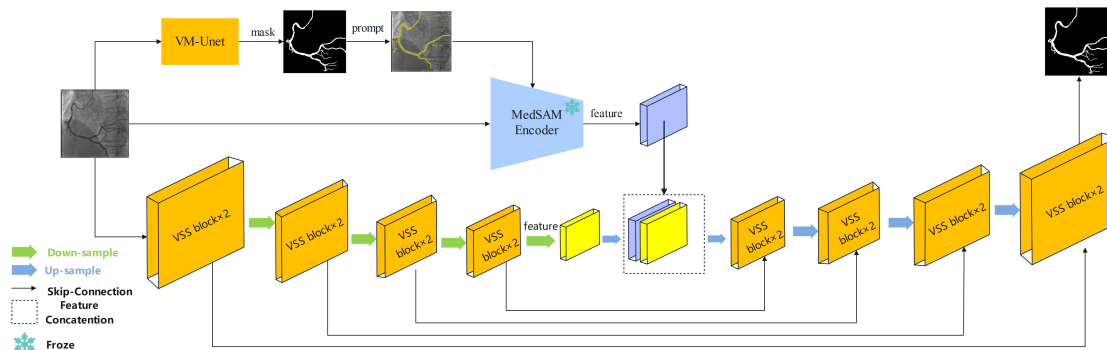


Figure 1: Schematic diagram of the SAM-VMNet framework

The architecture of our proposed SAM-VMNet framework is shown in Figure 1, which combines the technical advantages of MedSAM and VM-UNet. Specifically, SAM-VMNet has two parallel encoders, where MedSAM is a widely used macromodel in the field of medical image segmentation and VM-UNet is a new architecture based on visual state space blocks. This makes it possible not only to take advantage of MedSAM’s strong feature extraction capability, but also to speed up inference by taking advantage of VM-UNet’s ability to establish long-distance dependencies while maintaining linear complexity. Since MedSAM requires strong cues, we first trained a simple VM-UNet to coarsely segment the

image, and subsequently selected 10 points at equal spacing on the masked image as cues to be fed back to MedSAM, thus automatically obtaining the feature vectors output from the MedSAM encoder. The feature vectors from the two encoders are concatenated and fed into the decoder of the VM-UNet to finally obtain the output mask image. MedSAM, being a plug-and-play plug-in, has its parameters frozen during the training process, and only the weights of the VM-UNet are continuously updated during the training process.

## II.B. VM-UNet

Vision Mamba Uet (VM-UNet) is the first medical image segmentation model based purely on State Space models (SSM). The model employs an asymmetric encoder-decoder structure and introduces visual state space (VSS) blocks to capture a wide range of contextual information, resulting in excellent performance in medical image segmentation tasks.

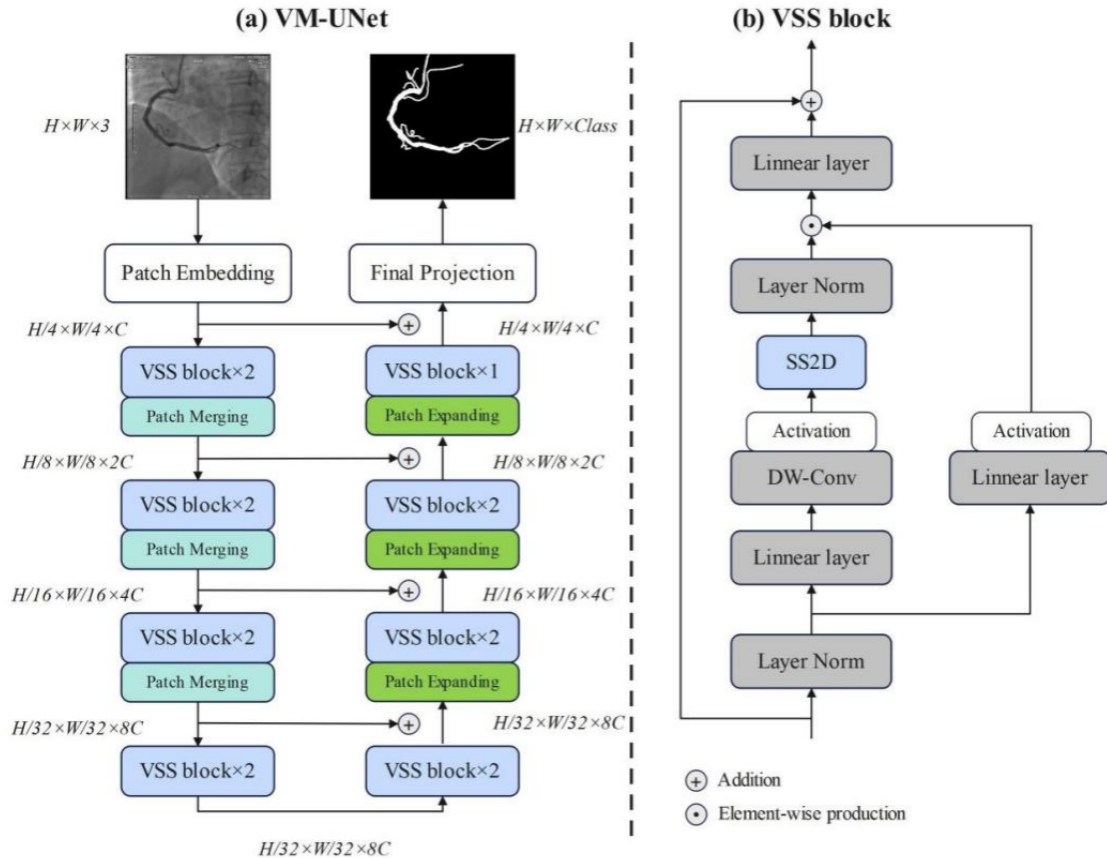


Figure 2: (a) VM-UNet general architecture; (b) VSS block is the main building block of VM-UNet, and SS2D is the core operation in the VSS block

Figure 2(a) illustrates the general architecture of VM-UNet, specifically, VM-UNet consists of a Patch Embedding layer, an encoder, a decoder, a Final Projection layer, and skip connections. The Patch Embedding layer divides the The input image  $x \in \mathcal{R}^{H \times W \times 3}$  is divided into non-overlapping patches of size, and subsequently maps the image into C-dimensional.

This process will produce an image embedding  $x' \in \mathcal{R}^{\frac{H}{4} \times \frac{W}{4} \times C}$ . Finally, we normalize the input encoder using Layer Normalization before subjecting it to feature extraction. The encoder consists of four stages, with a Patch merge operation applied at the end of the first three stages to reduce the height and width of the input features while increasing the number of channels. Each of the four stages uses a  $[2, 2, 2, 2]$  VSS block with a channel count of  $[C, 2C, 4C, 8C]$  for each stage. The decoder is similarly divided into four stages. At the beginning of the last three stages, the patch expanding operation is used to reduce the number of feature channels and increase the height and width of feature channels. In the four stages,  $[2, 2, 2, 1]$  VSS blocks (asymmetric architecture) are used with channel counts of  $[8C, 4C, 2C, C]$  in each stage. After the decoder, a Final Projection layer is used to recover the size of the features to match the segmentation target. Specifically, the height and width of the features are recovered by 4 up-sampling through patch expansion, and then the number of channels is recovered through the projection layer. For hopping connections, the addition operation is used directly so that no additional parameters are introduced.

The VSS block is derived from VMamba, which is the core module of VM-UNet, as shown in figure 2(b). The input is divided into two branches after Layer Normalization. In the first branch, the input passes through a linear layer and an activation function. In the second branch, the input is processed through a linear layer, a depth-separable convolution and an activation function, and then fed into the 2D-Selective-Scan (SS2D) module for further feature extraction. Subsequently, the features are normalized using Layer Normalization and then the two paths are merged. Finally, the features are blended using Linear Layers and this result is combined with the residual join to form the output of the VSS block.

The most basic binary cross-entropy and dice loss (BceDice loss) and cross-entropy and dice loss (CeDice loss) in VM-UNet are used as loss functions for two- and multi-class segmentation tasks:

$$L_{\text{BceDice}} = \lambda_1 L_{\text{Bce}} + \lambda_2 L_{\text{Dice}} \quad (1)$$

$$L_{\text{CeDice}} = \lambda_1 L_{\text{Ce}} + \lambda_2 L_{\text{Dice}} \quad (2)$$

$$L_{\text{Bce}} = -\frac{1}{N} \sum_{i=1}^N [y_i \log(\hat{y}_i) + (1 - y_i) \log(1 - \hat{y}_i)] \quad (3)$$

$$L_{\text{Ce}} = -\frac{1}{N} \sum_{i=1}^N \sum_{c=1}^C y_{i,c} \log(\hat{y}_{i,c}) \quad (4)$$

$$L_{\text{Dice}} = 1 - \frac{2|X \cap Y|}{|X| + |Y|} \quad (5)$$

Where:  $N$  is the total number of samples,  $C$  is the total number of categories;  $y_i, \hat{y}_i$  and denote the true label and prediction, respectively; is an indicator equal to 1 if sample  $i$

belongs to category  $c$ , and 0 otherwise;  $y_{i,c}^{\hat{}}$  is the probability that the model predicts that sample  $i$  belongs to category  $c$ ;  $|X|$  and  $|Y|$  denote the true value and prediction, respectively;  $\lambda_1, \lambda_2$  is the weights for the loss function, and the default value is 1 for both.

## II.C. Parallel network architecture

MedSAM is the first base model designed for general-purpose medical image segmentation based on the Vision Transformer architecture with three main components: an image encoder, a cue encoder, and a mask decoder. And by fine-tuning it to achieve optimal performance on multiple medical image segmentation tasks on a dataset of more than one million publicly available medical images, the architecture has been shown to have extremely strong feature extraction capabilities. To combine the powerful feature extraction capabilities of MedSAM, we first trained a simple VM-Unet to coarsely segment the images to obtain boundary cues suitable for MedSAM. Therefore, SAM-VMUnet employs two parallel network structures to extract image features. Specifically, the image input is passed through the VM-UNet of branch 1 to obtain a coarse segmentation image, on which 10 points are chosen at equal spacing as the prompts for MedSAM to obtain the feature vector  $x_1 \in \mathcal{R}^{1 \times 256 \times 64 \times 64}$ . The image input is passed through the VM-UNet encoder of branch 2 to obtain the feature vector  $x_2 \in \mathcal{R}^{1 \times 8 \times 8 \times 768}$ . Downsampling of  $x_1$  with  $1 \times 1$  convolution and average pooling layer makes  $x_1$  dimension consistent with  $x_2$  dimension for further feature fusion.  $x_1, x_2$  feature fusion by simple summation. This process makes reasonable use of MedSAM’s cue encoder, which generates high-quality feature vectors. The fused vectors are then up-sampled by VM-UNet’s decoder to finally output the predictions. During the backpropagation training process, only the weights of the VM-UNet in branch 2 are continuously updated, while the weights of MedSAM and the simple VM-UNet in branch 1 are frozen, which allows them to be used as plug-and-play feature extraction plug-ins.

## III. Experimental Setting

Several datasets were used in this study, including a private dataset and the publicly available ARCADE dataset. The private dataset was approved by China Guihang Group 302 Hospital and contains a total of 25 annotated coronary angiography image segmentation datasets, of which 15 were used for training and 10 for testing. The ARCADE dataset<sup>19</sup> contains 1200 annotated coronary vascular tree images divided according to the training set (1000 images) and validation set (200 images). Each training image is annotated with 26 different regions labelled according to the Syntax Score method [20].

Regarding dataset usage, first we used the private dataset for coarse segmentation of VM-UNet, based on `vmamba_small_e238_ema` pre-training with fine-tuning on the weights. We used the ARCADE dataset for the learning of the backbone network SAM-VMNet; in the MedSAM model, we used `medsam_vit_b` as the initial weights for feature acquisition.

For the training of the network, we based our implementation on Pytorch and trained it

on an NVIDIA GeForce 4090 graphics card. 200 epochs were set, seed was 42, batch was 32, drop rate was 0.2, and the initial learning rate was 0.001, The AdamW optimisation strategy was used for optimisation, and the loss function was the same as that of VM-UNet, using binary cross entropy and Dice loss.

Among the evaluation metrics, we chose mIoU, dice, accuracy, specificity, and sensitivity.

The mIoU is a performance metric commonly used to evaluate image segmentation tasks. First, the ratio of the intersection of the predicted region and the real region to their concatenation is calculated, and after calculating the intersection and concatenation ratios for each category, the average of these values is taken as the mIoU. The higher the value of the mIoU, the better the segmentation result matches the real situation. The calculation formula is as follows:

$$\text{mIoU} = \frac{\text{TP}}{\text{TP} + \text{FP} + \text{FN}} \tag{6}$$

The dsc can be used to assess the similarity of two samples. It is calculated as the size of the intersection of the twice predicted and true results divided by the total size of both. The calculation formula is as follows:

$$\text{dice} = \frac{2\text{TP}}{\text{TP} + \text{FP} + \text{FN}} \tag{7}$$

The accuracy shows the ability of the model to correctly identify all categories. It is calculated by dividing the number of all correctly categorised pixels by the total number of pixels. The formula is as follows:

$$\text{accuracy} = \frac{\text{TP} + \text{TN}}{\text{TP} + \text{TN} + \text{FP} + \text{FN}} \tag{8}$$

Specificity measures the proportion of all negative samples that are correctly identified as negative by the model, with higher values indicating that the model seldom misclassifies negative samples as positive; sensitivity measures the proportion of all positive samples that are correctly identified as positive by the model, with higher values indicating that the model captures all positive samples well. The formula is as follows:

$$\text{specificity} = \frac{\text{TN}}{\text{TN} + \text{FP}} \tag{9}$$

$$\text{sensitivity} = \frac{\text{TP}}{\text{TP} + \text{FN}} \tag{10}$$

## IV. Results

### IV.A. Training results on 1500 images dataset

In order to evaluate the segmentation performance of SAM-VMNet for coronary angiography images, we selected popular deep learning networks for medical image segmentation: unet, unet++<sup>20</sup>, transunet<sup>21</sup>, malunet<sup>22</sup>, transfuse<sup>23</sup>, missformer<sup>24</sup> and our proposed network and the original VM-UNet for comparison, using the same dataset as well as preprocessing strategies, and computing the segmentation metrics as shown in Table 1.

Table 1: Assessment indicators for model comparisons

Method	mIoU	Acc	Spe	Sen	Dice
<b>UNet</b>	51.53%	96.56%	52.26%	53.25%	55.23%
<b>UNet++</b>	58.56%	98.08%	76.47%	71.43%	73.87%
<b>TransUNet</b>	43.64%	97.62%	75.69%	51.41%	58.89%
<b>MALUNet</b>	55.61%	98.01%	99.15%	68.01%	71.47%
<b>Transfuse</b>	57.37%	97.69%	98.19%	85.11%	72.10%
<b>Missformer</b>	23.81%	96.93%	68.63%	27.04%	36.80%
<b>VM-UNet</b>	54.45%	97.73%	98.86%	69.87%	70.51%
<b>SAM-VMNet</b>	<b>63.03%</b>	<b>98.32%</b>	<b>99.33%</b>	73.43%	<b>77.33%</b>

The table 1 shows the model segmentation performance on 1500 number of coronary image data. Among all the models, SAM-VMNet outperforms other models in mIoU, Acc, Spe, F1 evaluation metrics, which shows that SAM-VMNet has a significantly competitive performance, and our model outperforms Transunet, which is based on Transformer, as well as MALUNet. The experimental results also show the superiority of SSM model in the field of medical image segmentation.

The results show that SAM-VMNet performs extremely well on coronary artery image segmentation, and effectively improves the generalisation ability and performance of the model by integrating the pre-trained MedSAM encoder into the VM-Unet framework. proposed network can both take advantage of the powerful feature extraction capability of MedSAM and also plays a role in the VM-Unet ability to capture contextual information. The experiments on coronary artery image segmentation show the superiority over other models. over state-of-the-art models such as Transunet, MALUnet and Transfuse. Compared to SAM, SAM-VMNet can be optimised for semantic segmentation of medical images using VM-Unet, which improves the accuracy of image segmentation. Our study shows that with a multi-head design, SAM-VMNet learns shape prior simultaneously during end-to-end training, and no longer needs to train a separate network to encode image information, the model combining multiple segmentation frameworks can effectively improve the accuracy of medical image segmentation, and the fusion of features extracted from different modules further increases the richness of the features, which allows the model to better perform the segmentation task.



## V. Discussion

The results demonstrate the superior performance of SAM-VMNet for medical image segmentation. By integrating a pre-trained SAM encoder into the VM-UNet framework, SAM-VMNet exploits MedSAM’s powerful feature extraction capabilities on medical images while benefiting from VM-UNet’s long-range modelling capabilities. On the publicly available coronary vascular dataset, SAM-VMNet consistently maintains the highest accuracy across a variety of tasks, outperforming advanced models such as Missformer, UNet++, and TransUNet, and maintains the highest specificity, which demonstrates that our model is highly effective in identifying non-target regions.

In contrast to nnSAM<sup>25</sup>, we perform a coarse segmentation via a fine-tuned VM-UNet that provides cue points for MedSAM to obtain feature vectors instead of embeddings. This approach better utilises the powerful feature extraction capability of MedSAM and is more conducive to extracting the vessel region of interest. Our study demonstrates that SAM-VMNet, which combines the Transformer and Mamba segmentation frameworks, can effectively further improve the accuracy of medical image segmentation. In addition, since VM-UNet maintains linear complexity, it is able to reduce the consumption of arithmetic operations, thus improving the computational efficiency.

## VI. Limitation

Although SAM-VMNet performs well in medical image segmentation, there are still some limitations that need to be further explored and improved.

Firstly, the memory of SSM is inherently lossy, so it is not as good as the lossless memory of the attention mechanism. Mamba is unable to show its advantages in processing short sequences, so some local features or small areas of structure in the image may be lost, but this is an area where the attention mechanism happens to perform well.

Second, in terms of cue point selection, although the method of using a fine-tuned VM-UNet for rough segmentation and generating cue points performed well in our study, the effectiveness of this method may be affected by the quality of the initial segmentation results. If the initial segmentation results are not accurate enough, it may affect the effectiveness of the subsequent MedSAM feature extraction and thus the final segmentation results.

Finally, although our method performs well on the coronary vascular dataset, its ability to generalise to other types of medical image segmentation tasks needs further validation. Different types of medical images have different features and challenges, therefore, evaluation on a wider range of medical image datasets is needed to fully validate the generalisation and stability of SAM-VMNet.

## VII. Conclusion

We propose a novel network architecture, SAM-VMNet, which fully combines the powerful feature extraction capability of MedSAM with the ability of VM-UNet to establish long-range dependencies while maintaining linear complexity. With this combination, SAM-VMNet achieves high-quality segmentation of coronary angiography images for the case of multi-branched coronary vessels. Our experimental results show that SAM-VMNet performs well in medical image segmentation tasks, outperforming current state-of-the-art models in terms of accuracy and specificity. In the future, we plan to further optimise the model and validate it in a wider range of medical image segmentation tasks with a view to enhancing its generality and usefulness.

## References

- <sup>1</sup> W. H. Organization, *World Health Statistics 2021: Monitoring Health for the SDGs, sustainable development goals*, World Health Organization, Geneva, Switzerland, 2021.
- <sup>2</sup> S. Moore, Pathogenesis of atherosclerosis, **34**, 13–16 (1985).
- <sup>3</sup> H. Lars, L. Sebastian, D. Lotus, S. Tiziano, G. Oliver, S. Burkhardt, C. Philippe, F. Thomas, T. G. Flohr, and M. Borut, Coronary artery motion and cardiac phases: dependency on heart rate – implications for CT image reconstruction, *Radiology* **245**, 567–576 (2019).
- <sup>4</sup> M. Paulinas, D. Miniotas, M. Meilūnas, and A. Ušinskas, An Algorithm for Segmentation of Blood Vessels in Images, *Elektronika ir Elektrotechnika* **93**, 25–32 (2015).
- <sup>5</sup> F. Orujov, R. Maskeliunas, R. Damasevicius, and W. Wei, Fuzzy logic based vessel segmentation in angiograms for CAD diagnosis, *Journal of Medical Imaging and Health Informatics* **10**, 1–8 (2020).
- <sup>6</sup> S. Eiho, H. Sekiguchi, N. Sugimoto, T. Hanakawa, and S. Urayama, Branch-based region growing method for blood vessel segmentation, (2004).
- <sup>7</sup> P. Makowski, T. S. Sørensen, S. V. Therkildsen, A. Materka, H. Stødkilde-Jørgensen, and E. M. Pedersen, Two-phase active contour method for semiautomatic segmentation of the heart and blood vessels from MRI images for 3D visualization, *Computerized Medical Imaging and Graphics* **26**, 9–17 (2002).
- <sup>8</sup> J. F. Carrillo, M. Hernández Hoyos, E. E. Dávila, and M. Orkisz, Recursive tracking of vascular tree axes in 3D medical images, *International Journal of Computer Assisted Radiology and Surgery* **1**, 331–339 (2007).

- <sup>9</sup> R. Manniesing, M. A. Viergever, and W. J. Niessen, Vessel axis tracking using topology constrained surface evolution., *IEEE Transactions on Medical Imaging* **26**, 309–316 (2007).
- <sup>10</sup> R. Phellan, A. Peixinho, A. Falco, and N. D. Forkert, Vascular Segmentation in TOF MRA Images of the Brain Using a Deep Convolutional Neural Network, (2017).
- <sup>11</sup> O. Ronneberger, P. Fischer, and T. Brox, U-Net: Convolutional Networks for Biomedical Image Segmentation, *arXiv preprint arXiv:1505.04597* (2015).
- <sup>12</sup> A. Kirillov, E. Mintun, N. Ravi, H. Mao, C. Rolland, L. Gustafson, T. Xiao, S. Whitehead, A. C. Berg, W.-Y. Lo, P. Dollár, and R. Girshick, Segment Anything, (2023).
- <sup>13</sup> A. Dosovitskiy, L. Beyer, A. Kolesnikov, D. Weissenborn, and N. Houlsby, An Image is Worth 16x16 Words: Transformers for Image Recognition at Scale, (2020).
- <sup>14</sup> J. Ma, Y. He, F. Li, L. Han, C. You, and B. Wang, Segment anything in medical images, *Nature Communications* **15** (2024).
- <sup>15</sup> A. Gu and T. Dao, Mamba: Linear-Time Sequence Modeling with Selective State Spaces, (2023).
- <sup>16</sup> J. Ruan and S. Xiang, VM-UNet: Vision Mamba UNet for Medical Image Segmentation, (2024).
- <sup>17</sup> S. Yang, J. Kweon, J. H. Roh, J. H. Lee, and S. J. Park, Deep learning segmentation of major vessels in X-ray coronary angiography, *Scientific Reports* **9**, 16897 (2019).
- <sup>18</sup> M. Nobre Menezes, J. Lourenço-Silva, B. Silva, T. Rodrigues, A. R. G. Francisco, P. Carrilho Ferreira, A. L. Oliveira, and F. J. Pinto, Development of deep learning segmentation models for coronary X-ray angiography: Quality assessment by a new global segmentation score and comparison with human performance, *Revista Portuguesa de Cardiologia* **41**, 1011–1021 (2022).
- <sup>19</sup> M. Popov, A. Amanturdieva, N. Zhaksylyk, A. Alkanov, A. Saniyazbekov, T. Aimyshev, E. Ismailov, A. Bulegenov, A. Kolesnikov, A. Kulanbayeva, A. Kuzhukeyev, O. Sakhov, A. Kalzhanov, N. Temenov, and S. Fazli1, ARCADE: Automatic Region-based Coronary Artery Disease diagnostics using x-ray angiography imagEs Dataset Phase 1, 2023.
- <sup>20</sup> Z. Zhou, M. M. R. Siddiquee, N. Tajbakhsh, and J. Liang, UNet++: A Nested U-Net Architecture for Medical Image Segmentation, (2018).
- <sup>21</sup> J. Chen, Y. Lu, Q. Yu, X. Luo, and Y. Zhou, TransUNet: Transformers Make Strong Encoders for Medical Image Segmentation, (2021).
- <sup>22</sup> J. Ruan, S. Xiang, M. Xie, T. Liu, and Y. Fu, MALUNet: A Multi-Attention and Light-weight UNet for Skin Lesion Segmentation, 2022.

- <sup>23</sup> Y. Zhang, H. Liu, and Q. Hu, TransFuse: Fusing Transformers and CNNs for Medical Image Segmentation, (2021).
- <sup>24</sup> S. Becker, R. Hug, W. Hübner, M. Arens, and B. T. Morris, MissFormer: (In-)attention-based handling of missing observations for trajectory filtering and prediction, 2021.
- <sup>25</sup> Y. Li, B. Jing, Z. Li, J. Wang, and Y. Zhang, nnSAM: Plug-and-play Segment Anything Model Improves nnUNet Performance, 2024.